PHYSICAL REVIEW B VOLUME 44, NUMBER 7 15 AUGUST 1991-I

Method of determining tip structure in atomic force microscopy

Sun M. Paik, Sihong Kim, and Ivan K. Schuller
Physics Department, B-0319 University of California, San Diego, La Jolla, California 92093-0319
(Received 8 February 1991; revised manuscript received 12 April 1991)

The stability of single atomic tip is tested using molecular-dynamics simulation. Many metallic single-atomic tips are unstable during the scan at a tip load well below typical experimental values. For the bcc W(111) tip, second-layer-tip-atomic contributions are comparable to the first-layer contribution. These results suggest that experimentally multiple-atom tips are involved in the scanning process. We propose a method to identify tip size and structure during the scanning process. The resultant images for a number of commonly used tip materials are interpreted and compared to experiments.

Since the first scanning tunneling microscope (STM) introduced by Binning and Rohrer,[1] other similar techniques, such as the atomic force microscope (AFM) and the magnetic force microscope (MFM),[2] have demonstrated the ability to probe surface topography with atomic resolution. While these devices provide much interesting surface topographical information, quite often a variety of anomalous images are obtained.[1,2] These anomalous images have been explained based on multiple-tip effects[3,4] and surface charge density calculation.[5] Despite much recent theoretical interest, these phenomena are not well understood yet. Moreover, it is difficult to verify experimentally which effects dominate in a particular experimental situation. In this paper, we present a systematic study of tip dynamics, and propose a method to identify size and structures of tips.

Ideally, a single-atomic-tip apex will provide the best atomic resolution. However, there are many situations in which multiple atoms may be involved in an actual scan. In the AFM, the scanning tip is brought into close proximity with the surface at a distance (of the order of an Å) at which the typical tip-surface interaction energy (of the order of an eV) (Ref. 6) is comparable to a typical metal-metal interaction energy (of the order of 0.1 eV).[7] Because of this large tip-surface interaction, a single-atomic-tip apex may be unstable during the scan, and multiple-atom tips may be involved in the scanning process even if a single-atomic tip is prepared initially. In fact, modification of the tip structure as well as substrate material has been observed in an earlier numerical study.[8] Experimentally, it is difficult to monitor directly the detailed tip structure during the scanning process. Thus a detailed theoretical investigation of single-atomic-tip stability is very important. Also, for certain tip materials [for example, the W(111) tip which is commonly used in experiments][9] the contribution of second-layer-tip atoms is comparable to that of top-layer atoms, when local surface deformation is present. In these situations, multiple-tip effects must be taken into account in order to interpret the experimental data correctly.

The purpose of this paper is to investigate the stability of a single-atomic metallic tip, to study atomic relaxation effects at finite temperatures, and to develop a method for analyzing tip structure during the scan by using the relative rotational dependence of images. As an example, we study the graphite surface which has served as a prototype material for demonstrating atomic resolution. To be specific, we simulate images produced by the atomic force microscope, although, we believe that the general features discussed below are valid for other types of scanning microscopes. We first investigate the stability of a single-atom tip and atomic relaxation effects at finite temperature, using the molecular-dynamics (MD) simulation technique. We find that a single-atom tip is permanently damaged with a tip-surface interaction force ($\approx 4\times10^{-9}$ N for Ni and $\approx 7\times10^{-9}$ N for Pt tips) which is order of magnitude smaller than tip loads in experiments conducted in air or vacuum.[10] The tip deforms at a force well before any significant surface deformation occurs.[4] In contrast with earlier studies in which tip deformation effects were neglected,[3-6] our results indicate that tip dynamics plays as important a role as other factors and must be considered in STM or AFM studies. For the W(111) tip, the contribution from the second-layer-tip atoms is comparable to that of the apex atom due to the elastic surface deformation at finite temperatures. In this situation, the tip size in the second layer is also important. All the situations discussed above may complicate the interpretation of the images. Thus it is necessary to investigate systematically the tip structure effects on the image. For this reason, we have studied the relative orientation dependence of the AFM images which gives, as we will show below, information about the tip structure. Using Fourier analysis methods, we are able to identify the size and structure of the tip by investigating the change in force and topology of the images as a function of relative tip orientation. These results are in good agreement with the earlier experiment and the numerical model calculation.[11] Although the MD studies depend explicitly on the details of the interaction potentials, we must stress that the qualitative results are valid for other choices of the potentials such as the embedded-atom potential.[12] The static Fourier analysis, on the other hand, is independent of the details of the interaction potentials and only depends on the relative topology of the surface and tip.

To study tip stability and atomic relaxation effects, we employ the standard molecular-dynamics simulation technique[13] for three movable layers of graphite, support-

ed on a rigid substrate layer. A modified graphite potential, earlier developed by Abraham and Batra,[4] is used with a harmonic interlayer potential replacing the Lennard-Jones (LJ) potential, i.e., a harmonic potential for interlayer interaction and a Stillinger-Weber-type[14] three-body potential ($A=5.373\,203\,7$, $B=0.598\,245\,71$, $a=1.894\,361\,9$, $\lambda=18.707\,929$, and $\gamma=1.2$) for graphite intralayer interactions. The harmonic interlayer potential was introduced to obtain the correct stacking configuration of graphite with the force constant determined from the experimental C_{33} elastic constant.[7] We use the Lennard-Jones (12-6) potential with a cutoff at $r_c=2.5\sigma$ for tip-surface and tip-tip interactions with the potential parameters for tip-surface interaction chosen as an algebraic average of tip-tip and interlayer interaction graphite.

Figure 1 shows the tip load (force perpendicular to the surface) as a function of tip-surface distance (z) for Ni (dashed line) and Pt (solid line) tips. Both tips oriented along the (111) direction consist of 21 stationary atoms and 35 movable atoms. A single atom is placed at the tip apex and exhibits three exposed facets ($1\bar{1}\,\bar{1}$), ($\bar{1}1\bar{1}$), and ($\bar{1}\,\bar{1}1$). The temperature is controlled by rescaling the velocities of the first two movable layers (25 atoms). As the tip-surface distance decreases, the tip load increases until it reaches a critical load ($\approx 4\times10^{-9}$ and 7×10^{-9} N for the Ni and Pt tip, respectively). As the tip-surface distance decreases further, the load decreases sharply at the critical load, due to plastic deformation of the tip. This permanent tip deformation is confirmed by observing the actual atomic motion during the simulation. We have also observed that, frequently, the single-atomic-tip apex is damaged during lateral scanning (in the x,y direction at constant height) *even for lower tip loads.* These critical tip loads are one order of magnitude smaller than experimental loads and a numerical calculation of surface plastic deformation forces.[9] As in all MD simulations inaccuracies of the empirical potentials prevent us from deducing quantitative conclusions. However, considering that (1) the Lennard-Jones (LJ) potential between tip atoms contributes most significantly to the critical tip load, since the tip-surface interaction is in the repulsive core region and the carbon-carbon bonds strength are much stronger than tip-tip interaction; and (2) fcc metals are described fairly well by LJ potentials, we believe that our numerical findings are close to real critical tip loads. The possibility of tip instability in single-atom tips certainly must be taken into account in STM and AFM studies.

In order to investigate surface relaxation effects, we scan the graphite surface at rate of 0.0002 Å per MD time step, in constant height mode. Figure 2(a) shows a scanned image using a W(111) single atomic tip [consists of three facets (110), (101), and (011)] with an average tip load $F_t\approx3\times10^{-9}$ N, at room temperature. The W(111) tip geometry is one of the most common tip geometries used in experiments.[15] Since there is no empirical potential that stabilizes the bcc W structure, we employ a harmonic potential for the interatomic interaction between W atoms. The force constant is determined from the curvature of an empirical W interatomic potential[16] at the energy minimum. In contrast to rigid atomic simulation in which a honeycomb image is found [Fig. 2(b)], a triangular image is observed at room temperature. At room temperature, the distance between the second-tip layer and surface atoms is smaller than for a rigid system due to surface elastic deformations. As the tip apex approaches the surface, the nearest surface region below deforms and as a consequence the contribution from the second layer on the tip (three atoms in this case) becomes comparable to that of the single-apex atom. This was checked by calculating the contribution to the force from each individual layer. Since all four atoms, in the first and the second layer, are involved in the scanning process at finite temperatures, the image may also depend on the orientation of the tip. We note that the second-layer contribution may also be large when the tip scans near small surface vacancy sites. For the fcc (111) tips (Ni and Pt), second-layer contributions are negligible because of the larger interlayer distance on the tip.

These dynamical simulations suggest that experimentally the scanning tips are most likely polyatomic and that the surface topology may be modified by the scanning tip. It is important therefore to ascertain whether it is possible to measure the tip structure during the scan. Experimentally, it is almost impossible to measure the tip structure directly, and moreover, the tip may be modified by the tip-surface interaction. However, as we will show

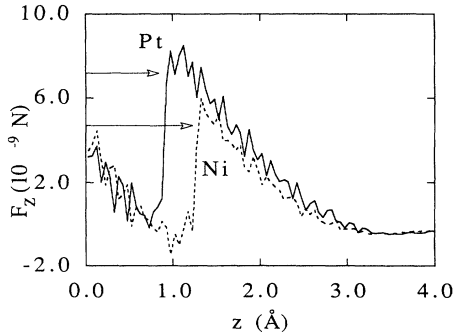

FIG. 1. Tip load (F_z) as a function of tip-surface distance (z) for single-atomic Ni tip (dashed line) and Pt tip (solid line). The arrows indicate the critical tip load for each tip.

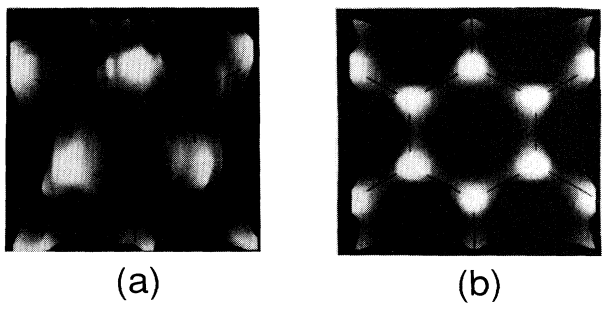

FIG. 2. Scanning images using W(111) tip with single atom on the tip apex: (a) with surface relaxation at room temperature; and (b) without surface relaxation in the rigid model calculation.

here, it is possible to identify *indirectly* the tip size and structure by analyzing the orientation dependence of images. One advantage of this method is that it is independent of the details of the interaction potentials and depends only on the symmetry of the system.

In a periodic structure such as the graphite surface, the tip-surface interaction force (tunneling current in STM) (Ref. 3) can be written as a Fourier series,

$$F_z=\sum_{\mathbf{G}}F_{\mathbf{G}}(z)\sum_{j}^{N_{\rm tip}}e^{-i\mathbf{G}\cdot\mathbf{R}_j}=\sum_{\mathbf{G}}F_{\mathbf{G}}(z)e^{-i\mathbf{G}\cdot\mathbf{R}_0}\xi_{\mathbf{G}}(\theta,\rho)\ , \quad (1)$$

where $\mathbf{G}$, $F_{\mathbf{G}}$, $N_{\rm tip}$, $\mathbf{R}_j$, $\mathbf{R}_0$, θ, and ρ are surface reciprocal lattice vectors of graphite, Fourier components of the interaction force, number of tip atoms, two-dimensional position vectors of tip atoms, position vector of the origin of tip axes, relative tip orientation, and lattice constant ratio of tip and surface material. At high temperatures, atomic relaxation reduces the periodicity of the surface lattice and makes Eq. (1) inapplicable. Moreover, this approach is not applicable to nonperiodic samples. The information regarding tip structure is contained in the tip structure factor,

$$\xi_{\mathbf{G}}(\theta,\rho)=\sum_{j=1}^{N_{\rm tip}}e^{-i\mathbf{G}\cdot\mathbf{R}'_j}\ , \quad (2)$$

which is a function of relative orientation and lattice constant ratio, where $\mathbf{R}'_j$ is a relative position of tip atoms with respect to the origin of tip axis $\mathbf{R}_0$. Equation (2) implies that, as far as the force results are concerned, the relative positions of tip atoms are only important within a reciprocal lattice vector of the imaged *substrate*. One intuitive way of looking at this is to reflect all tip atoms into one unit cell of the substrate ("effective tip"). It is easy to understand that if this effective tip covers a small area of the substrate unit cell, an atomic resolution image may be obtained. In general, the effective tip size depends on the number of atoms on the tip, the relative orientations, and relative atomic sizes.

For the graphite surface, only three Fourier terms dominate Eq. (2), and higher-order terms decay rapidly.[3] This structure factor, in general, is a complex quantity and can be written in terms of an amplitude and phase shift, i.e., $\xi_{\mathbf{G}}(\theta,\rho)=r_{\mathbf{G}}(\theta,\rho)e^{i\phi_{\mathbf{G}}(\theta,\rho)}$ for all three $\mathbf{G}$'s. The image depends on both amplitude and phase shift. However, only one quantity of the three phase shifts, i.e., $\varphi(\theta,\rho)\equiv\phi_1(\theta,\rho)+\phi_2(\theta,\rho)+\phi_3(\theta,\rho)$, will change the image distinctively; the other two degrees of freedom will only shift the image translationally, since the different choices (two degrees of freedom) of the tip origin (origin of the rotation) only shift the image.

Different choices of the amplitudes $r_{\mathbf{G}}(\theta,\rho)$ and the $\varphi(\theta,\rho)$ generate all five topologically distinct images of a graphite surface that are found in experiments and STM calculation using Fourier analysis.[3] If all three amplitudes $r_{\mathbf{G}}(\theta,\rho)$ are comparable and the phases $\varphi(\theta,\rho)=0$, the honeycomb lattice will be imaged. For instance, if a single tip atom is involved in the scanning process, $r_{\mathbf{G}}(\theta,\rho)$ and φ are 1 and 0 (independent of θ and ρ), respectively, for all three $\mathbf{G}$'s. If $\varphi=\pi/2$, a triangular array of triangles will be imaged. A triangular array of spheres will be imaged for $\varphi=\pi$. If the amplitudes of the two Fourier components dominate the third, the image will be a triangular array of ellipses. On the other hand, if one dominates the other two, a bandlike strip image will show up.

Figure 3 shows $r_{\mathbf{G}}(\theta,\rho)$ (solid lines) and $\varphi(\theta,\rho)$ (dashed lines) as a function of the relative tip orientation for Pt(111) tips of (a) a triangular tip shape (three atoms); and (b) a rhombic shape (four atoms). The corresponding images at four different relative orientations $\theta=0°$, 10°, 20°, and 30° are presented in Fig. 4 where the relative orientation is defined by the angle between a surface lattice constant vector and a lattice constant vector of tip material. The images with triangular tip [Fig. 4(a)] vary from honeycomb at $\theta=0°$ to a triangular array of triangles at intermediate θ, to a triangular array of spheres at $\theta=30°$ (this image may not be observed in experiments due to small amplitudes and rapid angular variance of φ at $\theta\approx30°$). Note that it is not possible to obtain either the

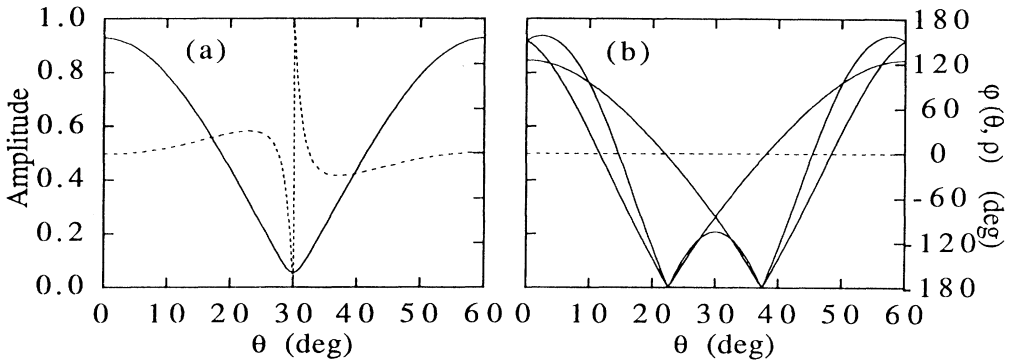

FIG. 3. Amplitude (solid lines) and phase (dashed line) of the tip structure factor as a function of tip orientation for (a) a three atom triangular Pt tip; and (b) a four atom rhombic Pt tip. The y axes in the left represent the amplitudes and the right sides the phase.

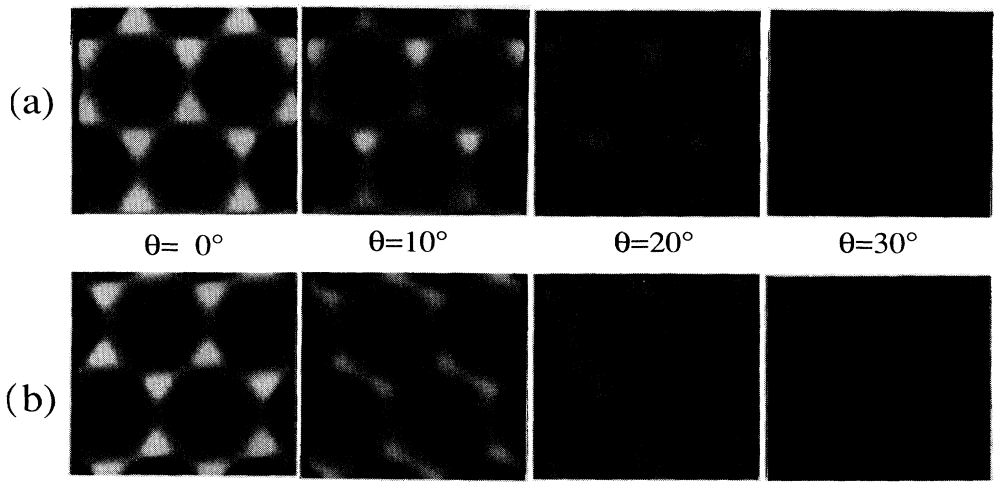

FIG. 4. Scanning images corresponding to Fig. 3 at $\theta=0°$, 10°, 20°, and 30°.

strip image or a triangular lattice image of ellipses with a triangular shape of the tip, because the amplitudes of the three Fourier components are always the same at all the relative orientations. The amplitudes $r_G(\theta,\rho)$ are peaked at $\theta=0°$, 60°, 120°, . . . , and their peak values are about 0.9, i.e., the force per atom with a polyatomic tip at $\theta=0°$ is 0.9 times that of the single-atom tip. The width of these peaks depends on the number of tip atoms that are involved in the scanning process and the lattice constant ratio between surface and tip materials. On the other hand, for the four atoms rhombic tip [Figs. 3(b) and 4(b)], the amplitudes of the three Fourier components are different from each other but $\varphi=0$ for all θ. Thus the triangular array of triangles or spheres is not possible in this case. The amplitudes of the all three Fourier components are comparable at $\theta\approx 0°$ and, thus, a honeycomb lattice will be imaged. As the orientation increases, a triangular array of ellipses at $\theta\approx 10°$ and a strip image at $\theta\approx 20°$ will be obtained. These results are in good agreement with the earlier experiment and the numerical model calculation.[11]

As the tip size increases, the width of the amplitude peak decreases with tip orientation (i.e., the atomic force decreases faster with increasing orientation for a larger tip than for a smaller tip). For instance, the amplitude half width of a 10 atoms triangular tip is $\Delta\theta\approx 20°$ while $\Delta\theta\approx 40°$ for a three atoms tip. With a similar method used in the finite-size-dependent interfacial energy calculation on lattice mismatched system,[17] we can show that the peak width is approximately proportional to $1/\eta_G\rho$ where η_G is the size of the tip along **G**. Thus a measurement of the signal intensity (or relative force corrugation) reflects also the size of the tip. In practice, it may be difficult to measure relative corrugation changes due to inaccuracy of experimental data and changes in the tip from scan to scan. Thus accurate prediction of the number of tip atoms may be difficult. However, it may be possible to measure the geometrical tip structure since observations of the pattern sequences (for instance, "honeycomb" to "triangular lattice of triangle" images or "honeycomb" to "triangular lattice of ellipses" to "strip" images) may still be observable. This is also supported by the fact that many of these images have been observed in a number of laboratories. Of course, if the tip geometry and shape change continuously from run to run the method described here may not be useful.

We have also investigated other tip shapes. For example, for a double tip, the image changes from a honeycomb to a triangular array of ellipses to the strip images as the relative orientation changes from $\theta=0°$ to 30°. For a seven atom hexagonal tip, there will be only two topologically distinct images, a honeycomb and a triangular array of triangles. The intensity of image goes to zero at $\theta\approx 21°$. For the W(111) tip, the general features are the same as the Pt tip but the honeycomb structure maximum amplitude peaks (where the honeycomb lattice is imaged) show up at every 30° instead of every 60° as for Pt and Ni tips. More detailed results will be published elsewhere.[18]

In summary, we have studied atomic force microscopy using molecular-dynamics simulation and the Fourier analysis technique. We have investigated the stability of single-atom-metallic tip and atomic relaxation effects at finite temperature using molecular dynamics. We found that single-atomic Ni and Pt tips were damaged permanently at a few nanonewtons of tip load during the scanning procedure due to tip-surface interaction. The elastic surface deformation effects are prominent for the W(111) tip but for other fcc metallic tips (Ni and Pt) this effect is very small. We have also studied the relationship between tip structure and scanned image using Fourier analysis. We showed that topological image changes can be used as an indirect measurement of the tip geometrical structure and the intensity of the signal (force corrugation) for measurement of the tip size.

We would like to thank R. Brandt for useful conversations. This work is supported by ONR, Grant No. N00014-91-J-1177 and Supercomputer time was provided by the University of California–San Diego Supercomputer Center.

[1]G. Binning and H. Rohrer, Physics **127B**, 37 (1984); G. Binning, H. Fuchs, Ch. Gerber, H. Rohrer, E. Stoll, and E. Tosatti, Europhys. Lett. **1**, 31 (1986).

[2]G. Binning, C. F. Quate, and Ch. Gerber, Phys. Rev. Lett. **56**, 930 (1987); O. J. Marti, B. Drake, and P. K. Hansma, Appl. Phys. Lett. **51**, 484 (1987); see also, for example, various articles in the Proceedings of STM'90/NANO I, edited by R. J. Colton, C. R. K. Marrian, and J. A. Stroscio, J. Vac. Sci. Technol. B **9**, 401 (1991).

[3]H. A. Mizes, Sang-il Park, and W. A. Harrison, Phys. Rev. B **36**, 4491 (1987); I. P. Batra, N. Garcia, H. Rohrer, H. Salemink, E. Stoll, and S. Ciraci, Surf. Sci. **181**, 126 (1987).

[4]S. Ciraci and I. P. Batra, Phys. Rev. B **36**, 6194 (1987); I. P. Batra and S. Ciraci, J. Vac. Sci. Technol. A **6**, 313 (1988); F. F. Abraham and I. P. Batra, Surf. Sci. **L125**, 209 (1989). S. A. C. Gould, K. Burke, and P. K. Hansma, Phys. Rev. B **40**, 5363 (1989).

[5]A. Selloni, P. Cornevali, E. Tosatti, and C. D. Chen, Phys. Rev. B **31**, 2602 (1985); **34**, 7406 (1986).

[6]G. Overney, W. Zhong, and D. Tomanek, J. Vac. Sci. Technol. B **9**, 479 (1991).

[7]T. Halicioglu and G. M. Pound, Phys. Status Solidi **30**, 619 (1975); *Handbook of the Physiochemical Properties of the Elements,* edited by G. V. Samsonov (IAI/Plenum, New York, 1968), p. 387.

[8]Uzi Landman, W. D. Luedtke, and M. W. Ribarsky, J. Vac. Sci. Technol. A **7**, 2829 (1989).

[9]H. Wengelnik and H. Neddermeyer, J. Vac. Sci. Technol. A **8**, 438 (1990).

[10]T. R. Albrecht and C. F. Quate, J. Appl. Phys. **62**, 2599 (1987). However, some experiments in liquid have been done at much lower tip loads. A. L. Weisenhorn, P. K. Hansma, T. R. Albrecht, and C. F. Quate, Appl. Phys. Lett. **54**, 2651 (1989).

[11]R. J. Colton, S. M. Baker, R. J. Driscoll, M. G. Youngquist, and Baldeschwieler, J. Vac. Sci. Technol. A **6**, 349 (1988).

[12]For a recent review, see M. Baskes, M. Daw, B. Dodson, and S. Foiles, Mater. Res. Soc. Bull **13**, 28 (1988); M. I. Baskes, Phys. Rev. Lett. **59**, 2666 (1987); E. T. Chen, R. N. Barnett, and Uzi Landman, Phys. Rev. B **40**, 924 (1989).

[13]A. Rahman, Phys. Rev. A **136**, 405 (1964); J. P. Hansen and L. Verlet, *ibid.* **184**, 151 (1969).

[14]F. H. Stillinger and T. Weber, Phys. Rev. B **31**, 5262 (1985).

[15]H. Wengelnik and H. Neddermeyer, J. Vac. Sci. Technol. A **8**, 438 (1990).

[16]W. F. W. M. van Heugten and J. Th. M. de Hosson, Phys. Status Solidi B **90**, 225 (1978).

[17]Sun M. Paik and Ivan K. Schuller, Phys. Rev. Lett. **64**, 1923 (1990); **66**, 395(E) (1991).

[18]Sun. M. Paik, Sihong Kim, and Ivan K. Schuller (unpublished).

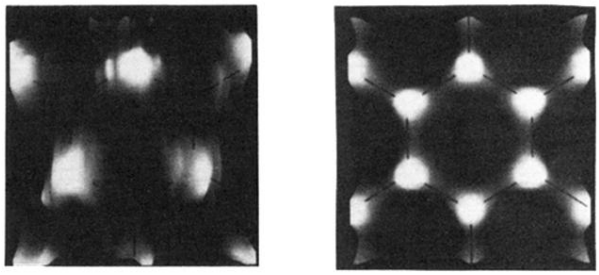

FIG. 2. Scanning images using W(111) tip with single atom on the tip apex: (a) with surface relaxation at room temperature; and (b) without surface relaxation in the rigid model calculation.

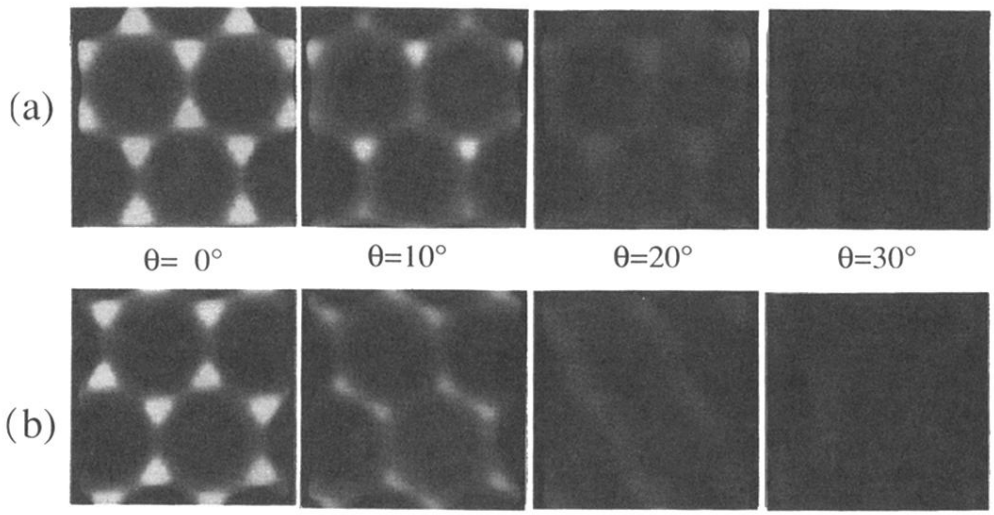

FIG. 4. Scanning images corresponding to Fig. 3 at $\theta=0°$, 10°, 20°, and 30°.